




RESEARCH ARTICLE

High heat tolerance, evaporative cooling, and stomatal decoupling regulate canopy temperature and their safety margins in three European oak species

Alice Gauthey^{1,2,3}  | Ansgar Kahmen⁴ | Jean-Marc Limousin⁵ | Alberto Vilagrosa⁶ | Margaux Didion-Gency⁷ | Eugénie Mas^{1,2,8}  | Arianna Milano^{1,2} | Alex Tunas^{1,2,9} | Charlotte Grossiord^{1,2} 

¹Plant Ecology Research Laboratory PERL, School of Architecture, Civil and Environmental Engineering, EPFL, Lausanne, Switzerland

²Community Ecology Unit, Swiss Federal Institute for Forest, Snow and Landscape Research WSL, Birmensdorf, Switzerland

³Birmingham Institute of Forest Research, University of Birmingham, Birmingham, UK

⁴Physiological Plant Ecology, Department of Environmental Sciences, University of Basel, Basel, Switzerland

⁵Centre d'Ecologie Fonctionnelle et Evolutive, CNRS, EPHE, IRD, Université de Montpellier, Montpellier, France

⁶CEAM Foundation, Joint Research Unit University of Alicante-CEAM, Department Ecology, University of Alicante, Alicante, Spain

⁷Forest Dynamics Unit, Swiss Federal Institute for Forest, Snow and Landscape WSL, Birmensdorf, Switzerland

⁸Forest Global Earth Observatory, Smithsonian Tropical Research Institute, Washington, District of Columbia, USA

⁹Department of Ecology, University of Innsbruck, Innsbruck, Austria

Correspondence

Alice Gauthey, Plant Ecology Research Laboratory PERL, School of Architecture, Civil and Environmental Engineering, EPFL, Lausanne CH-1015, Switzerland. Email: a.gauthey@bham.ac.uk

Funding information

Schweizerischer Nationalfonds zur Förderung der Wissenschaftlichen Forschung, Grant/Award Number: 310030_204697; Analyses et Expérimentations pour les Ecosystèmes, Grant/Award Number: ANR-11-INBS-0001; INERTIA, Grant/Award Number: PID2019-111332RB-C22

Abstract

Heatwaves and soil droughts are increasing in frequency and intensity, leading many tree species to exceed their thermal thresholds, and driving wide-scale forest mortality. Therefore, investigating heat tolerance and canopy temperature regulation mechanisms is essential to understanding and predicting tree vulnerability to hot droughts. We measured the diurnal and seasonal variation in leaf water potential (Ψ), gas exchange (photosynthesis A_{net} and stomatal conductance g_s), canopy temperature (T_{can}), and heat tolerance (leaf critical temperature T_{crit} and thermal safety margins TSM, i.e., the difference between maximum T_{can} and T_{crit}) in three oak species in forests along a latitudinal gradient (*Quercus petraea* in Switzerland, *Quercus ilex* in France, and *Quercus coccifera* in Spain) throughout the growing season. Gas exchange and Ψ of all species were strongly reduced by increased air temperature (T_{air}) and soil drying, resulting in stomatal closure and inhibition of photosynthesis in *Q. ilex* and *Q. coccifera* when T_{air} surpassed 30°C and soil moisture dropped below 14%. Across all seasons, T_{can} was mainly above T_{air} but increased strongly (up to 10°C > T_{air}) when A_{net} was null or negative. Although trees endured extreme T_{air} (up to 42°C), positive TSM were maintained during the growing season due to high T_{crit} in all species (average T_{crit} of 54.7°C) and possibly stomatal decoupling (i.e., $A_{\text{net}} \leq 0$ while $g_s > 0$). Indeed, *Q. ilex* and *Q. coccifera* trees maintained low but positive g_s (despite null A_{net}), decreasing

This is an open access article under the terms of the [Creative Commons Attribution-NonCommercial-NoDerivs](https://creativecommons.org/licenses/by-nc-nd/4.0/) License, which permits use and distribution in any medium, provided the original work is properly cited, the use is non-commercial and no modifications or adaptations are made.

© 2024 The Author(s). *Global Change Biology* published by John Wiley & Sons Ltd.

Ψ passed embolism thresholds. This may have prevented T_{can} from rising above T_{crit} during extreme heat. Overall, our work highlighted that the mechanisms behind heat tolerance and leaf temperature regulation in oak trees include a combination of high evaporative cooling, large heat tolerance limits, and stomatal decoupling. These processes must be considered to accurately predict plant damages, survival, and mortality during extreme heatwaves.

KEYWORDS

canopy temperature, critical leaf temperature, drought, heatwave, oak, photosynthesis, water potential

1 | INTRODUCTION

Anthropogenic activities have already induced a warming of global mean average surface temperatures of 1.2°C above preindustrial levels (1850–1900), and global temperatures are further expected to rise by 0.2°C per decade (IPCC, 2023). Through the modulation of land-atmosphere feedback, high air temperatures (T_{air}) increase the vapor pressure deficit (VPD), in turn enhancing the severity of soil drought via higher evapotranspiration (Eamus et al., 2013; Grossiord et al., 2020; Will et al., 2013). The combination of atmospheric and soil droughts has led to widescale leaf scorching (Gong & Hao, 2023), a decline in forest productivity (Williams et al., 2013), and increased vegetation mortality across the globe (Hammond et al., 2022). However, while much attention has been given to the direct impacts of soil drought on plant functions, the mechanisms of heat stress remain more elusive. To prevent thermal damage during hotter droughts, trees must endure high T_{air} by keeping their leaves' temperatures (T_{leaf}) under a specific threshold which can vary seasonally to support physiological processes and avoid critical overheating. Yet, the physiological mechanisms governing heat tolerance, the regulation of canopy temperature during hot droughts, and how they differ among species growing in distinct biomes remain unclear as they have rarely been assessed, especially in the field.

In environments regularly exposed to heatwaves, where leaf damage (e.g., cell death) can occur within minutes (Hüve et al., 2011), high heat tolerance is critical for plant survival. Heat tolerance limits are usually quantified by measuring the temperature-induced drop in initial chlorophyll fluorescence F_o (i.e., the leaf critical temperature, T_{crit}). T_{crit} corresponds to the initial collapse of the photosystem II and the disruption of the electron's pathway, which is typically followed by leaf necrosis and death (Krause et al., 2010). T_{crit} is generally higher in tree species growing in warmer climates (Kitudom et al., 2022; O'sullivan et al., 2017) because of genetic variation and local acclimation, for example, via the induction of heat shock proteins, changes in leaf fatty acid composition, and antioxidant compounds stabilizing cell membranes (Coast et al., 2022; Lancaster & Humphreys, 2020). Locally, phenotypic plasticity can also increase heat tolerance, as shown for a wide range of tropical and temperate

broadleaf evergreen saplings exposed to manipulative conditions (Marchin et al., 2022; Sastry et al., 2018). Similarly, T_{crit} can acclimate across seasons (T_{crit} in summer > T_{crit} in winter; Zhu et al., 2018). Nevertheless, while T_{crit} provides key information about the specific temperature at which damage occurs at a given time (Cook et al., 2024), it does not inform on the actual thermal conditions experienced by vegetation in natural environments and needs to be associated with leaf temperature measurements to better understand heat tolerance mechanisms.

The in situ and dynamic variability in heat tolerance between species and biomes can be assessed with the thermal safety margin (TSM; the difference between T_{crit} and maximum T_{leaf}). When the TSM is exceeded (i.e., $T_{\text{leaf}} > T_{\text{crit}}$), vegetation will suffer from irreversible tissue damage, leading to severe dysfunctions and local tree mortality (Esperon-Rodriguez et al., 2021; Marchin et al., 2022). Few studies have tracked plant TSM in nature, but the few that have made these measurements suggested that TSM varies rapidly in function of local environmental conditions (Kullberg et al., 2024). For instance, previous work conducted along broad soil moisture and temperature gradients showed that TSM was higher in moist habitats compared to arid locations (Curtis et al., 2016) because of trees' stronger potential to maintain low T_{leaf} with evaporative cooling (Cook et al., 2021; Moran et al., 2023). Indeed, to maintain T_{leaf} under detrimental thresholds and keep positive TSM, T_{leaf} can be regulated by increasing latent heat loss through transpiration and evaporative cooling (Wilson et al., 2002). Hence, evaporative cooling is restricted when soil moisture is low, as drought leads to stomatal closure and reduces leaf cooling because of low leaf-level gas exchange to avoid xylem embolism (Bréda et al., 2006).

In contrast to the consistent drought impacts on gas exchange, stomatal behavior, and hence canopy cooling, effects under hot air are more complex, as evidenced by earlier research that shows a spectrum of reactions with rising T_{air} from stomatal opening (Marchin et al., 2016; Urban et al., 2017b) to closing (García-Forner et al., 2016). Maintaining stomata open under extreme temperatures could harm plants by increasing their water loss and cavitation risk (Schönbeck et al., 2022). Nevertheless, recent studies suggest that g_s and A_{net} , usually strongly correlated, may become decoupled

during heatwaves, such that g_s is maintained when A_{net} is reduced near to zero (De Kauwe et al., 2019; Drake et al., 2018; Marchin et al., 2023; Urban et al., 2017a). It was suggested that this decoupling under increased temperatures could be due to the decline in viscosity of H_2O at high temperatures, increasing its speed and fluidity, thus providing a water supply to the evaporative areas within the leaf intercellular cavities (Diao et al., 2024). In turn, it could result in passive latent heat dissipation, potentially enhancing leaf survival by avoiding lethal thermal damage induced by negative TSM. However, the underlying drivers of g_s and A_{net} decoupling are unclear but seem strongly associated with plant stomatal behaviour (Diao et al., 2024), whereby rather isohydric species (i.e., species with stronger stomatal closure during drought; Klein, 2014) show enhanced decoupling during heatwaves (Marchin et al., 2022, 2023). Nevertheless, no study has tracked the variation in stomatal opening, gas exchange, leaf temperature, and TSM in situ in mature forests along a range of species and biomes, limiting our understanding of tree thermal tolerance, species vulnerability to heat, and associated risks for forest dynamics.

In this study, we investigated how different oak species adapted to various ecological conditions regulate their stomatal opening, gas exchange, canopy temperature, and TSM daily and throughout the growing season. More specifically, we measured the diurnal and seasonal dynamics of leaf water potential (Ψ), net carbon and water exchange (A_{net} and g_s), canopy temperature (T_{can}), and heat tolerance (T_{crit} and TSM) in mature *Quercus coccifera*, *Quercus ilex*, and *Quercus petraea* trees along a latitudinal gradient in Europe (in Spain, France, and Switzerland, respectively). We hypothesized that (1) despite a potentially higher T_{crit} , the two southern species, *Quercus coccifera*, and *Quercus ilex*, should experience lower TSM due to the substantial g_s and Ψ reduction during the summer, reducing transpiration

and evaporative cooling and leading to high T_{can} . (2) In contrast, *Quercus petraea* that grows in a wetter region may have higher g_s that could help maintain transpiration and thus higher and positive TSM despite lower T_{crit} throughout the summer. (3) During the hottest and driest periods of the year, all species may open stomata and keep positive g_s , thus maintaining latent heat loss and avoid critical overheating.

2 | MATERIALS AND METHODS

2.1 | Sites description

The measurements were performed on three forest sites across Europe (Figure 1). The northern site is in Hölstein, Basel, Switzerland (47°26'19"N; 7°46'32"E; 550 m a.s.l.) at the Swiss-Canopy-Crane II (SCCII) research site (referred thereafter as CH). The site is a semi-natural, 100-year-old mixed temperate forest of the eastern Swiss Jura Mountains, which is co-dominated by European beech (*Fagus sylvatica* L.), Norway spruce (*Picea abies* L.), and natural deciduous hybrids at various percentage levels of Sessile oak (*Quercus petraea*) and Pedunculate oak (*Quercus robur*). For simplicity, we refer to these hybrids as *Quercus petraea* further in the text. The mean annual temperature (MAT) is 9°C and the mean annual precipitation sum (MAP) is 1009 mm. The stand density is ca. 300 stem ha⁻¹, the canopy height is approximately 32 m, and the basal area is 8.46 m² ha⁻¹. The 15 cm rock-free topsoil has a high clay content (over 40%), followed by varying inclusions of calcareous rocky material (15–30 cm) underlain by limestone bedrock. A 50-m tall canopy crane with a 62.5 m jib is installed in the center of the site and provided access to 312 trees from 10 species (see Kahmen et al., 2022 for more details about the

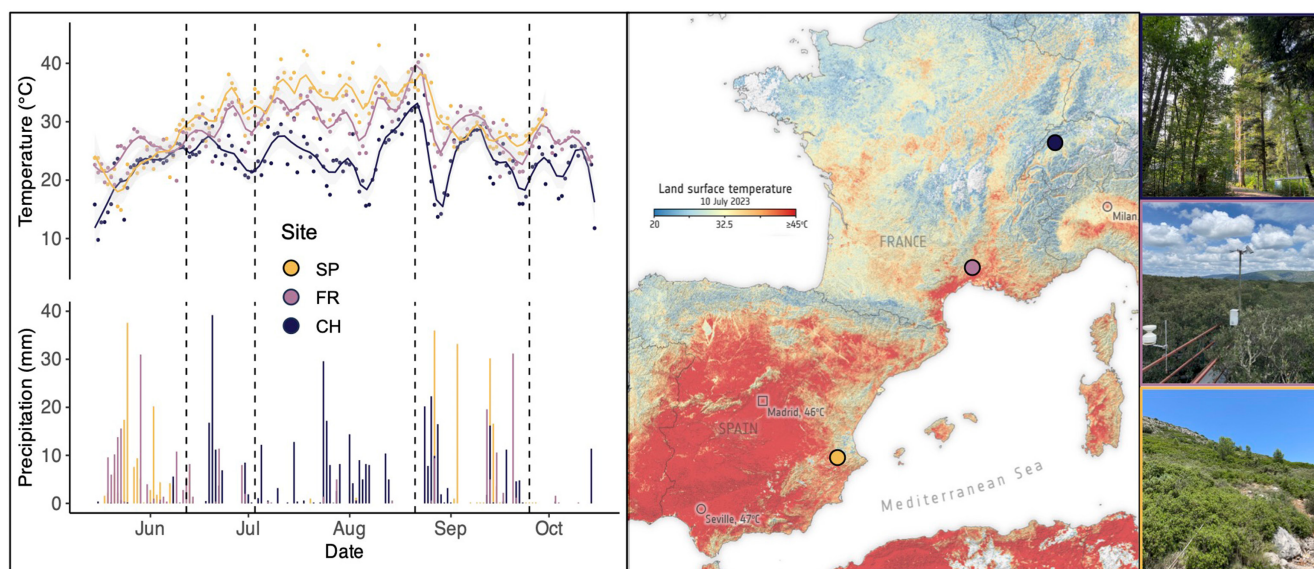


FIGURE 1 Left: Daily maximum temperature and total daily precipitation from May to November 2023. Dotted vertical lines indicate the start of our week-long four measurement campaigns for our three sites (SP: Dark blue, FR: Cyan, CH: Brown). Right: Map of Europe indicating the surface and pictures of each forest site.

site). Six dominant *Q. petraea* trees, which could be reached with the crane, were selected for this study and used for the leaf- and canopy-level physiological measurements (see below). *Q. petraea* represents the least drought-tolerant species included in this study with a water potential that induces 50% loss of conductivity (Ψ_{50}) of ~ -4.5 MPa (between -4.3 and -4.6 MPa from Lobo et al., 2018).

The intermediate site is in the Puéchabon national forest in the south of France, 35 km northwest of Montpellier ($43^{\circ}44'29''$ N; $3^{\circ}35'46''$ E, 270 m a.s.l.) (referred thereafter as FR), where an experimental site was setup in 2003. The forest is dominated by widespread Mediterranean evergreen oak *Quercus ilex* L. The climate is Mediterranean, characterized by a long summer drought, with a MAT of 13.8°C and a MAP of 965 mm (2008–2017, see Limousin et al., 2022 for more details about the site). The stand density is $4700 \text{ stem ha}^{-1}$, the canopy height is approximately 5.5 m, and the basal area is $29.5 \text{ m}^2 \text{ ha}^{-1}$. The soil is a silty clay loam filling the deep cracks on a limestone rock with a rooting depth of 4.5 m. We used two scaffolds, allowing us to reach the top of the canopy (20 m apart) to conduct the measurements, providing access to eight dominant *Q. ilex* trees ($n=4$ per scaffold). *Q. ilex* is a highly drought-tolerant species with a Ψ_{50} of ~ -7 MPa (-7.13 MPa from Lobo et al., 2018; between -6.6 and -7.2 MPa from Sergent et al., 2020).

The southern site is in the Valencian region in Spain, 56 km north of Alicante ($38^{\circ}48'35.5''$ N; $0^{\circ}27'30.8''$ W, 315 m a.s.l.) (referred thereafter as SP). The forest is a thermo-Mediterranean shrubland (Querco-Lentiscetum) dominated by the evergreen Kermes oak shrub (*Quercus coccifera*). The climate is semi-arid with a MAT of 18.2°C and a MAP of 277 mm (from Alicante-Elche airport weather station, www.aemet.es). The canopy height is approximately 1.5 m (allowing us to reach tree canopies without special equipment), and the ground cover is about 60% plants, 30% rock outcrops, and 10% bare soil. The soil is a calcareous limestone with abundant rock outcrops and basic pH with a depth of <30 cm. We selected eight dominant *Q. coccifera* shrubs in the field site for the measurements detailed below. Similar to *Q. ilex*, *Q. coccifera* is very drought-tolerant with a Ψ_{50} of ~ -7 MPa (Pita et al., 2005; Vilagrosa et al., 2003).

2.2 | Meteorological data

The CH site is equipped with 45 automated soil moisture probes (ML3 ThetaProbe; Delta-T Devices Ltd) installed at 14 locations across the site at 10, 40, and 80 cm soil depth. Temperature, relative humidity, wind speed, VPD, and solar radiation are recorded by a meteorological station installed on top of the crane (Davis Vantage Pro2; Davis Instruments Corp.). Data are measured every 5 min. The FR site is equipped with three soil moisture probes (ML2X ThetaProbe; Delta-T Devices Ltd) installed in the 0–6 cm soil layer and with six reflectometers (CS616-L Water Content Reflectometers; Campbell Scientific) installed in the 0–30 cm soil layer. The meteorological station is in a forest gap, 200 m away from the plot, and recorded air temperature (MP100 sensor; Rotronic), solar radiation (SKS1110; Skye Instruments), relative humidity, and

VPD at 2 m above ground. Precipitation was measured with a tipping bucket rain gauge (ARG100; Environmental Measurements) situated 1 m above ground. In the SP site, daily air temperature and relative humidity were taken from the closest weather station, approximately 10 km from our site (Muro d'Alcoi weather station, www.aemet.es). Hourly temperature, relative humidity, and VPD data were measured using our handheld temperature sensor on-site at the top of tree canopies (see below). Soil moisture was measured on-site in the 20 and 30 cm soil depth with eight soil moisture sensors (ECH20 EC5, Meter Group) connected to two dataloggers (Hobo 21-USB, Onset Computer Corporation).

It is important to note that, during our August campaign, air temperatures reached the second highest ever recorded values for our FR site (23 August, $T_{\text{air}} > 40^{\circ}\text{C}$) (Copernicus Climate Change Service/ECMWF, 2023). The other sites also experienced air temperatures and VPD slightly higher than long-term averages as well as substantial soil drying, but no extreme heatwave events were reported. All meteorological data are presented in Figure 1; Figure S1.

2.3 | Water potential and gas exchange

Four measurement campaigns of 1 day each were conducted in June, July, August, and September 2023 in the three sites. All campaigns were undertaken within 1 week during relatively cloudless days with each site measured on a different day. To determine stomatal regulation strategies, during each campaign, apical twigs of at least 5 cm in length were collected and stored in zip lock bags on the selected six (CH site) or eight (FR and SP sites) trees before sunrise (predawn) and every 2–3 h across the day (until sunset). After removing the bark on the excised part of the twig (to avoid false recording), water potentials (Ψ) were measured within 5–15 min with a Scholander-type pressure chamber (Model 1000, PMS Instrument Co.).

Gas exchange measurements were carried out using portable infrared gas analyzers (LI-6800, LI-COR Inc.) equipped with a 2 cm^2 leaf cuvette on attached sun-exposed leaves that had leafed out earlier the same year (for the two evergreen species in FR and SP sites). Different leaves on the same branches were used for water potential and gas exchange measurements. All leaves completely filled the cuvette. Repeated net photosynthesis (A_{net}) and stomatal conductance (g_s) measurements were taken under ambient temperature and humidity (measured continuously at each site with a portable RS PRO RS-91 Hygrometer, RS Components Ltd.), and ambient PAR (measured instantaneously before the measurements with the LI-6800 head). The reference CO_2 was set to 400 ppm. Measurements were done on leaves from the same branchlet (except for CH because of the difficulty of repeatedly reaching the same branches with the crane) every 2–3 h from sunrise to sunset and after steady-state gas exchange rates had been maintained for at least 2 min. Despite stabilization of A_{net} , g_s data were relatively noisy and we could not retrieve valid data for *Q. coccifera* in September. We extracted Ψ_{50} (i.e., water potential at which 50% conductivity is lost) xylem vulnerability curves from the literature (see above).

2.4 | Canopy temperature

During each campaign, we measured the canopy temperature (T_{can}) of each tree ($n=6$ or 8) with a drone equipped with an infrared camera. In June, thermal images were obtained using an uncooled infrared sensor (model DJI Zenmuse XT2) measuring between 7.5 and $13.5\ \mu\text{m}$ with a 640×512 pixel resolution mounted on a DJI M210 RTK V2 drone platform (DJI Technology Co, Ltd.). In June, only the FR and SP sites were measured because of technical failures of the drone at the CH site. Due to this issue, for the other campaigns, we used another uncooled thermal camera (model DJI Zenmuse H20T) measuring between 8 and $14\ \mu\text{m}$ with a 640×512 pixel resolution mounted on a DJI M300 RTK aircraft (DJI Technology Co., Ltd.). Considering the similarity between the two cameras, we do not expect this change to impact our results. During each campaign, 5–10 drone flights were executed from 8:00 a.m. to 7:00 p.m. at least 20 m above the tree canopy with 90% side and frontal frame overlaps. Drone flights took approximately 20–30 min and were conducted simultaneously with the physiological measurements (i.e., A_{net} , g_s and Ψ). We operated drone flights under a clear sky and low wind speed to minimize variations in acquisition geometry and associated noise. The thermal radiometric images collected with the XT2 camera were first converted to TIFF (32-bit) using FLIR Research Studio V 2.0 software (FLIR Systems Inc.) using an emissivity of 0.96 (Harrap et al., 2018). The images collected with the H20T camera were transformed to TIFF (32-bit) using code developed on GitHub (Kattenborn, 2023), changing the relative humidity for every flight to improve data accuracy. Images were georeferenced, geometrically calibrated, and assembled into ortho-mosaics using Agisoft PhotoScan (Agisoft LLC). In QGIS (QGIS c), individual tree canopies were manually delineated as polygons, and the average canopy temperature for each sampled tree was calculated using the zonal statistics plugin in QGIS. This plugin allows the user to calculate several values of the pixels of a raster layer within a polygonal vector layer.

To validate drone temperature ($T_{\text{plate-drone}}$), a custom-built black-painted (PNM400, Electrolube Ltd, United Kingdom) ventilated reference aluminum plate ($500\times 500\times 10\text{ mm}$) was installed at each field site during every campaign and recorded temperatures measured with a high-precision PT100 1/10 DIM resistance temperature sensor (GD-7124, Gräff GmbH, Germany) from the reference plate ($T_{\text{plate-sensor}}$). The relationship between $T_{\text{plate-drone}}$ extracted from drone images and $T_{\text{plate-sensor}}$ from the reference plate was estimated for every campaign and site ($R^2 > .98$) to correct canopy temperature accordingly.

2.5 | Critical leaf temperature and thermal safety margins

To assess heat tolerance, we measured the photosystem II response through the fluorescence degradation in leaves collected in June and July at our three sites. Leaves were measured using a PlanTherm PT100 (PSI, Drásov, Czech Republic), which measure the initial chlorophyll fluorescence to increasing temperature (F_0 - T curve). After sampling in the field, leaves were recut, avoiding the central vein,

when possible, to fit in the cuvette (2 cm long \times 1 cm large). The leaves were then immersed in the cuvette containing 5 mL of deionized water and heated slowly from 25 to 80°C at a rate of 2°C min^{-1} . A magnetic stirrer was used to achieve a homogenous temperature in the cuvette of the PlanTherm. While the temperature increases inside the cuvette, regular measurements of fluorescence are taken on the immersed leaf. The critical temperature (T_{crit}) given by the Plantherm is extracted from the thermotolerance curve as the temperature prior to the maximum acceleration of the fluorescence curve, similar to Gauthey et al. (2023).

Thermal safety margins (TSM) represent the thermal safety of the photosystem II and were calculated as follows for each tree and campaign:

$$\text{TSM} = T_{\text{crit}} - T_{\text{max}} \quad (1)$$

with T_{max} , the maximum canopy temperature of each tree recorded at each campaign.

Due to technical difficulties, we could not measure T_{crit} in August and September. However, because T_{crit} was very similar between June and July (see Section 3), we used the same mean T_{crit} to calculate TSM in August and September.

2.6 | Statistical analysis

The seasonal dynamics in Ψ , A_{net} , g_s , and T_{can} were analyzed for each species using a linear mixed-effect model (LMM, part of the lme4 package: Bates, 2010) where the campaign was used as a fixed effect, and the hour of measurement was incorporated as a random effect to account for repeated measurements on a single tree individual. After checking for normality, the diurnal dynamics of each species were analyzed using a repeated-measure ANOVA test for each month. All relationships between variables (A_{net} vs Ψ , A_{net} and g_s , T_{can} vs T_{air} , ΔT , and T_{air} , T_{can} vs A_{net}) were also analyzed with either a linear model (lm function) or a linear mixed-effect model (lme function). For A_{net} versus g_s , we pooled data from *Q. coccifera* and *Q. ilex*, which exhibited a similar pattern. To compare T_{crit} per site and TSM across species and per month, we used a one-way ANOVA followed by a Fisher's LSD (Least Significant Difference) test. All statistical analyses were performed using R (RStudio Team, 2015, v. 2023.12.0 + 369).

3 | RESULTS

3.1 | Seasonal and diurnal dynamics in leaf water potentials

A strong diurnal variation in Ψ was observed for all species (all $p < .05$), with high Ψ in the morning followed by a slow decrease until reaching the lowest Ψ in the afternoon (Figure 2). Moreover, all species had a clear seasonal variation in Ψ ($p < .05$) following the VPD dynamics (Figure S1), with the highest values at the start of the summer (in June)

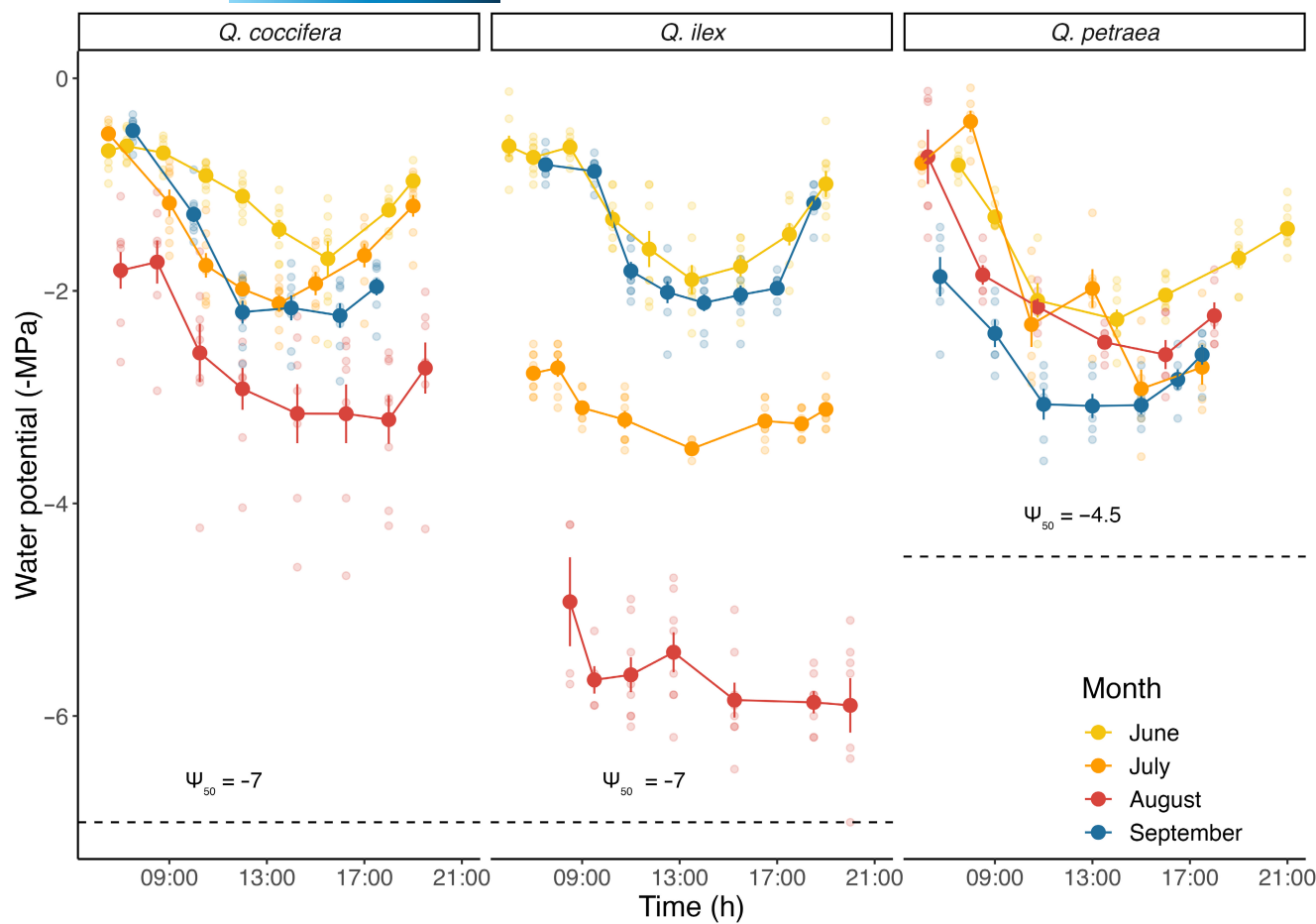


FIGURE 2 Diurnal and seasonal dynamics (yellow: June, orange: July, red: August, and blue: September) in leaf water potential in *Q. coccifera*, *Q. ilex*, and *Q. petraea*. Horizontal dotted lines represent species-specific Ψ_{50} . Data are means (\pm SE) of six (*Q. petraea*) to eight (*Q. coccifera* and *Q. ilex*) trees per species.

when VPD was the lowest and soil moisture the highest (daily average water potential Ψ_{avg} of -1.6 , -1.2 , and -1.0 MPa for *Q. petraea*, *Q. ilex*, and *Q. coccifera*, respectively). The lowest values for *Q. ilex* and *Q. coccifera* were found in August with Ψ_{avg} of -5.6 and -2.7 MPa, respectively. For *Q. petraea*, the lowest values were reached in September ($\Psi_{\text{avg}} = -2.7$ MPa) (Figure 2) possibly due to stress accumulation, early senescence, or because the fall was warm and dry.

Overall, *Q. ilex* experienced the lowest Ψ of all species, with the daily minimum Ψ dropping by 4 MPa between the June and August campaigns (from -1.9 to -5.9 MPa), which coincided with increasing air temperatures (daily maximum T_{air} from 24.9 to 41.4°C) and lower soil water availability (daily mean soil water content from 19.6% to 14.2%). Although *Q. coccifera* also had an important drop in minimum Ψ throughout the season, the range was limited to 1.5 MPa (from -1.7 to -3.2 MPa), with daily maximum T_{air} varying from 22.8 to 35.9°C and daily mean soil water content from 27% to 10% between June and August. *Q. petraea* experienced the least seasonal variation, with a difference in the minimum Ψ of only 0.8 MPa between June and September (from -2.3 to -3.1 MPa), with daily maximum T_{air} varying from 24.8 to 25.8°C and daily mean soil moisture between 30% and 25% between the campaigns at those months.

3.2 | Seasonal and diurnal dynamics in leaf-level gas exchange

Similarly to Ψ , a strong diurnal variation in A_{net} and g_s was found for all species ($p < .05$), increasing during the day before peaking in the late morning, followed by a decrease in the afternoon (Figure 3a,b).

For *Q. ilex* and *Q. coccifera*, the daily average of A_{net} (A_{avg}) was the highest in June (4.8 and $2 \mu\text{mol m}^{-2} \text{s}^{-1}$, respectively) and the lowest in August (-0.2 and $-1.1 \mu\text{mol m}^{-2} \text{s}^{-1}$, respectively), exhibiting negative values (photorespiration and mitochondrial respiration) most of the day. Similarly, for *Q. petraea*, A_{avg} was the highest in July ($10.8 \mu\text{mol m}^{-2} \text{s}^{-1}$) and lowest in August ($A_{\text{avg}} = 4.6 \mu\text{mol m}^{-2} \text{s}^{-1}$) but never exhibited negative values. Overall, *Q. petraea* had the highest annual average A_{net} of all species, followed by *Q. ilex* and *Q. coccifera* (6.6 , 2.5 , and $0.8 \mu\text{mol m}^{-2} \text{s}^{-1}$, respectively) (Figure 3a). Stomatal conductance followed a similar diurnal and seasonal pattern as A_{net} . Daily average g_s was the lowest in August for *Q. ilex* ($0.013 \text{ mol m}^{-2} \text{s}^{-1}$) and in August and September for *Q. petraea* (0.063 and $0.067 \text{ mol m}^{-2} \text{s}^{-1}$, respectively). Due to technical difficulties, g_s were not stable in the morning in SP in August and September, leading to overestimated g_s values. For *Q. coccifera*, in the afternoon, g_s

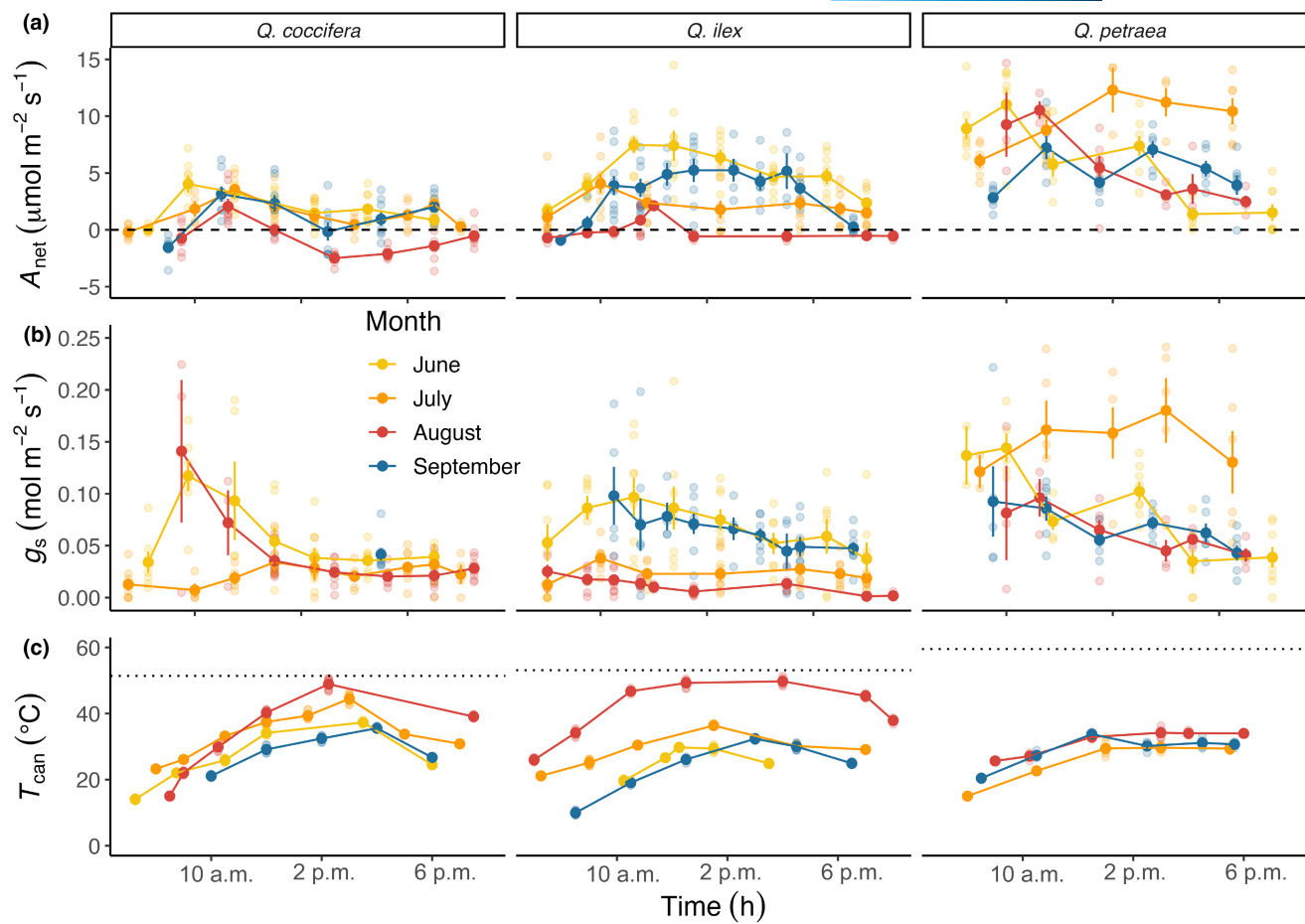


FIGURE 3 Diurnal and seasonal dynamics (yellow: June, orange: July, red: August, and blue: September) in net assimilation rate (a), stomatal conductance (b) and canopy temperature (c) in *Q. coccifera*, *Q. ilex*, and *Q. petraea*. Data are means \pm SE of six (*Q. petraea*) to eight (*Q. coccifera* and *Q. ilex*) trees per species. In (a), the dashed line represents the zero line and in (c), the dotted lines represent the species-specific T_{crit} (June and July).

ranged from $0.024 \text{ mol m}^{-2} \text{ s}^{-1}$ in August to $0.037 \text{ mol m}^{-2} \text{ s}^{-1}$ in June (Figure 3b).

In *Q. ilex* and *Q. coccifera*, we observed a significant positive relationship between A_{net} and g_s in June ($R^2 = .29$), July ($R^2 = .45$), and September ($R^2 = .36$) (all $p < .05$). However, this relationship was not significant in August ($R^2 = .04$, $p = .06$), wherein A_{net} was negative and g_s exhibited low but positive values (Figure 4a), suggesting a decoupling of A_{net} and g_s during the warmest and driest conditions. In *Q. petraea*, the relationships between A_{net} and g_s were strongly significant in all months except for July (Figure S2).

The relationship between g_s and Ψ was significant and positive for *Q. ilex* and *Q. coccifera* ($p < .01$) but not for *Q. petraea* ($p = .465$; Figure 4b). The absence of relationship suggests that *Q. petraea* did not experience severe drought stress, which would lower Ψ and induce a steep decrease in g_s . Similarly, but despite severe water stress, *Q. ilex* could sustain a positive g_s during times of low Ψ (lower than -4 MPa). In contrast, A_{net} was not maintained in *Q. ilex* and *Q. coccifera* when Ψ was below $\sim -5 \text{ MPa}$ and $\sim -3 \text{ MPa}$, respectively (Figure S3), except, in *Q. ilex* at 11 a.m., where all plants had an A_{net} of $\sim 2 \mu\text{mol m}^{-2} \text{ s}^{-1}$ (Figure S3).

3.3 | Seasonal and diurnal dynamics in canopy temperature

The two southern species (*Q. coccifera* and *Q. ilex*) had a similar diurnal and seasonal variation in canopy temperature whereby T_{can} increased in the morning until reaching its peak in the mid-afternoon (between 1 p.m. and 4 p.m.) before decreasing (Figure 3c). For these two species, T_{can} was the highest in August (reaching a daily maximum of 49.7 and 48.8°C , for *Q. ilex* and *Q. coccifera*, respectively), exceeding T_{air} by over 10°C , and the lowest in June (daily minimum of 14.0°C for *Q. coccifera*) and September (daily minimum of 9.9°C for *Q. ilex*). Similarly, T_{air} was highest in August in FR (41°C) and SP (41.1°C). *Q. petraea* showed similar diurnal dynamics but reached its T_{can} peak earlier, around 1 p.m., and did not decrease in the afternoon. For this species, there was no seasonal variation and T_{can} reached similar maxima of 29.6 , 34.2 , and 33.7°C from July to September, respectively (June was not measured) while maximum T_{air} were 33.7 , 29 , and 27°C for these months, respectively.

All T_{can}/T_{air} relationships were linear ($R^2 = .81$, $.90$, and $.46$ for *Q. coccifera*, *Q. ilex*, and *Q. petraea*, respectively) with T_{can} usually

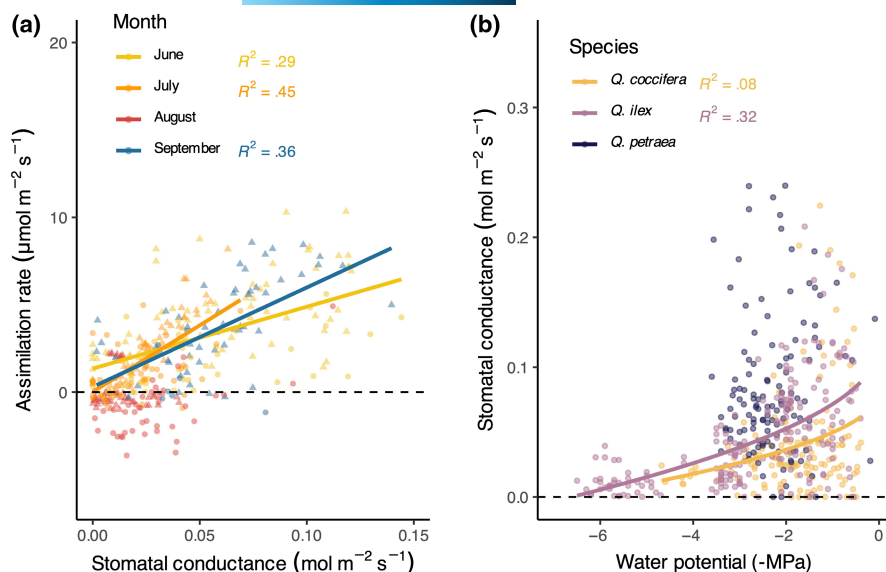


FIGURE 4 Relationships between the net assimilation rate and the stomatal conductance for pooled data from *Q. ilex* (triangle) and *Q. coccifera* (circle) for each field campaign (yellow: June, orange: July, red: August, and blue: September) (a). Relationships between stomatal conductance and leaf water potential for all field campaigns and species (yellow: *Q. coccifera*, pink: *Q. ilex*, dark blue: *Q. petraea*) (b). The R^2 indicates the significant relationships ($n=6-8$ trees per species).

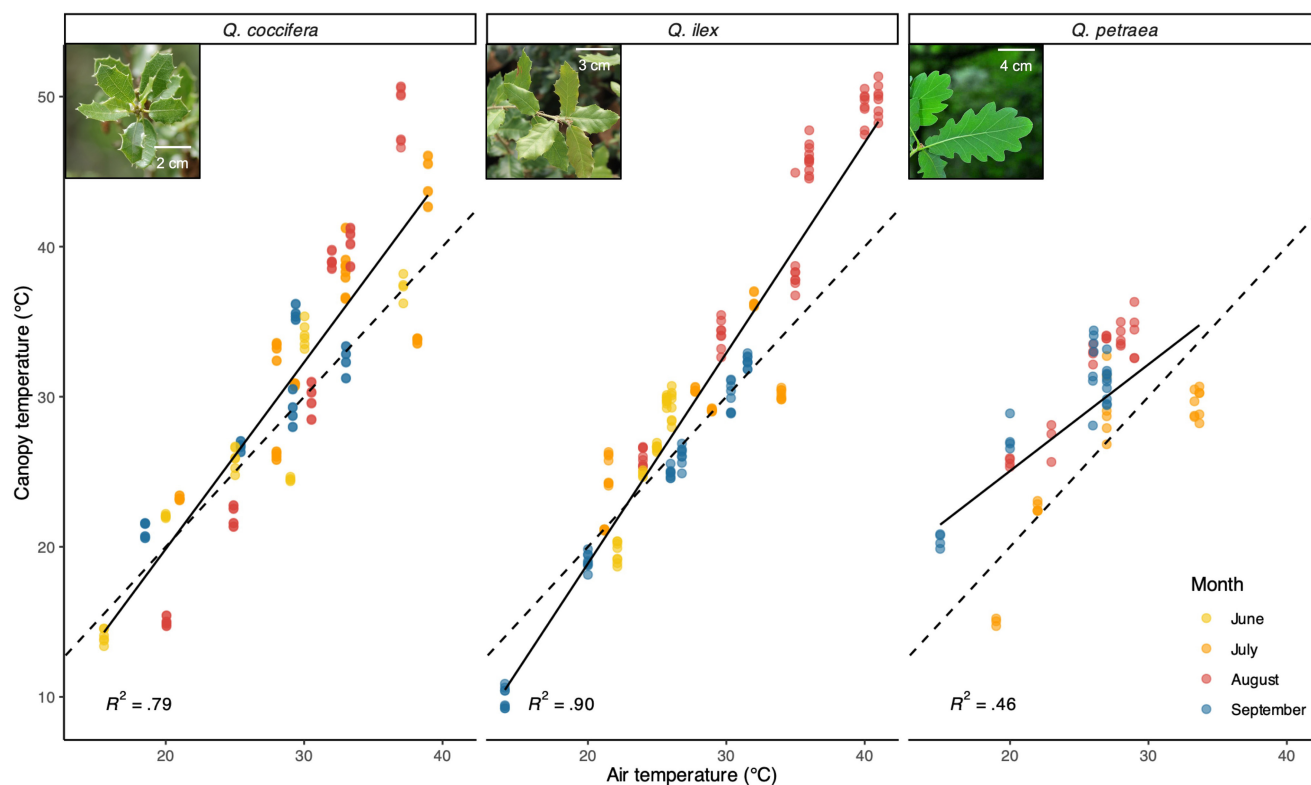


FIGURE 5 Relationships between the canopy and air temperatures across all months (yellow: June, orange: July, red: August, and blue: September) and hours of the day in *Q. coccifera*, *Q. ilex*, and *Q. petraea* ($n=6-8$ trees per species). The dashed line represents the 1:1 relationship, while the solid lines represent the relationship between T_{can} and T_{air} . The R^2 indicates the significant relationships.

above T_{air} during the daytime for all species (Figure 5). While for *Q. petraea*, T_{can} was rarely below T_{air} , we observed a counterclockwise hysteresis of this regression in *Q. coccifera* and *Q. ilex* whereby at low T_{air} (below 20°C), T_{can} was lower than T_{air} by a few degrees while at higher T_{air} , T_{can} was generally higher than T_{air} .

3.4 | Relationships between net gas exchange and canopy temperature

When the confounding effect of light incidence was removed (i.e., by removing data when the photosynthetic photon flux density was

below $500 \mu\text{mol m}^{-2} \text{s}^{-1}$), we found a significant negative relationship between the difference in T_{can} and T_{air} (ΔT , reflecting the canopy cooling through latent and sensible heat loss) and g_s for *Q. ilex* and *Q. petraea* ($p < .01$; Figure 6) and between ΔT and A_{net} for all species (Figure S4). Most times, ΔT was positive (i.e., T_{can} is warmer than T_{air}) and was the highest (lowest canopy cooling) when g_s was low or when A_{net} was close to 0 or negative. These relationships suggest that T_{can} regulation through evaporative cooling is only possible when soil water is high (e.g., in June and September) and when T_{air} was not extreme (lower than 30°C). We also observed a strong negative relationship between g_s and T_{can} ($R^2 = .19$, Figure S5) and A_{net} and T_{can} ($R^2 = .28$). This further indicates that T_{can} rises when A_{net} and g_s are reduced.

3.5 | Critical leaf temperature and thermal safety margins

The leaf critical temperature (T_{crit}) was significantly higher ($p < .05$) in *Q. petraea* (59.5°C) compared to *Q. ilex* (53.1°C) and *Q. coccifera* (51.4°C), which had similar T_{crit} ($p = .500$) (Figure 7c). Despite T_{can} increasing in the summer and resulting in decreasing thermal safety margins (TSM) for *Q.*

coccifera and *Q. ilex*, maximum T_{can} for all species did not exceed T_{crit} , resulting in positive TSM all along the growing season, even at the peak of summer (in August, average TSM $> 2^\circ\text{C}$) (Figure 7a). Moreover, we found a significant relationship between TSM and minimum water potential (Ψ_{min}) at each campaign for *Q. ilex* and *Q. coccifera* ($p < .01$; Figure 7b).

4 | DISCUSSION

Our study sheds new light on trees' vulnerability to heat by investigating the heat tolerance and canopy temperature regulation mechanisms of *Quercus* spp. in mature trees growing in contrasting biomes (from a temperate forest to a semi-arid woodland). We provided strong evidence that increased T_{air} and reduced soil moisture throughout the summer lead to warmer canopies, including severe overheating by up to 10°C above T_{air} during the hottest conditions in the southernmost sites (Figure 5). Thus, canopy temperature regulation was generally not efficient enough to lower T_{can} below T_{air} . However, despite negative A_{net} when daytime temperature surpassed $\sim 35^\circ\text{C}$, g_s was kept positive in the most southern species (Figures 3 and 4a), possibly due to stomatal decoupling. This decoupling, together with high heat tolerance and latent heat loss, allowed

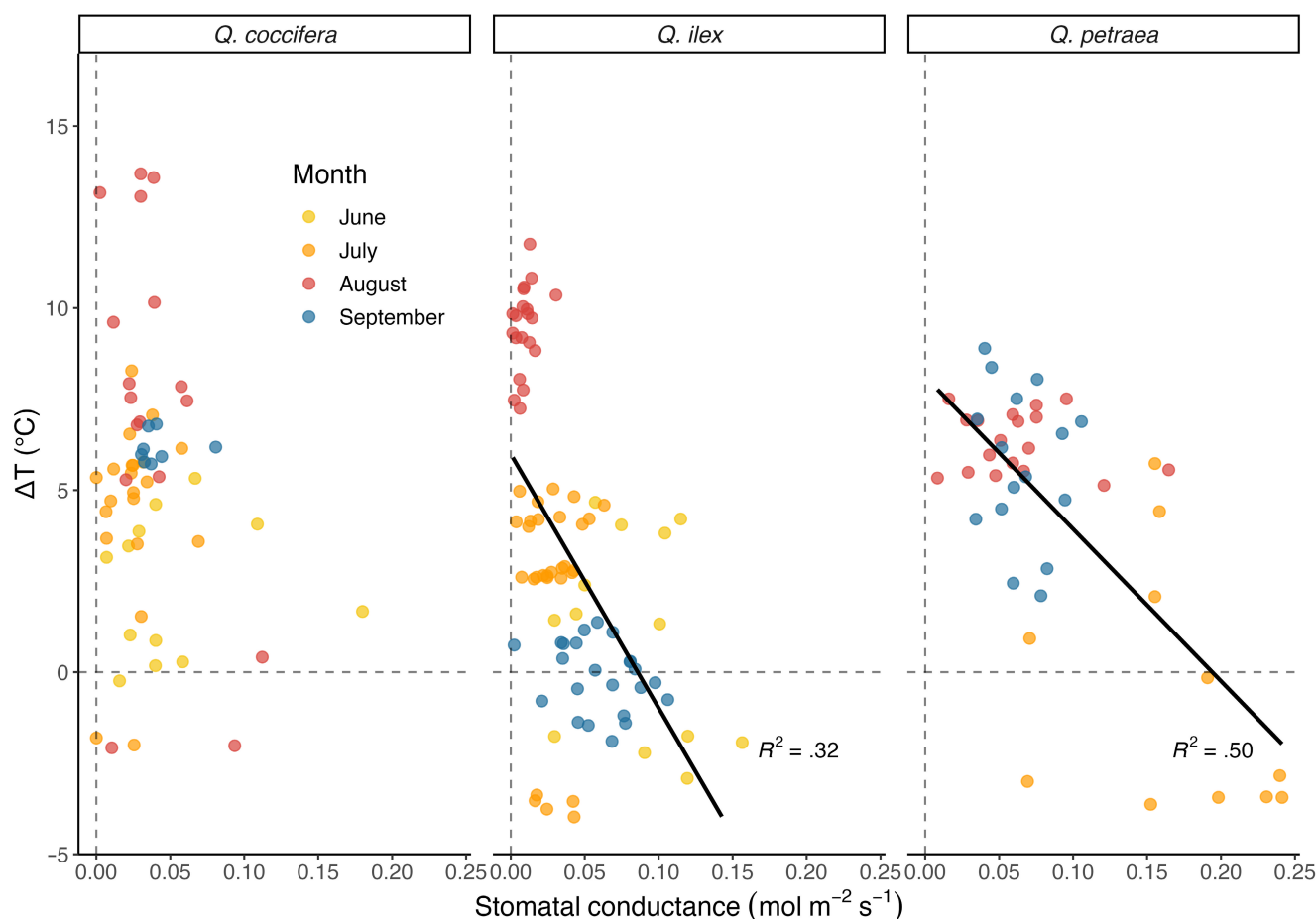


FIGURE 6 Relationships between the difference in the canopy and the air temperature (ΔT ; $T_{\text{can}} - T_{\text{air}}$) and the stomatal conductance across all months (yellow: June, orange: July, red: August, and blue: September) for *Q. coccifera*, *Q. ilex*, and *Q. petraea*. Data were taken when the photosynthetic photon flux density was above $500 \mu\text{mol m}^{-2} \text{s}^{-1}$. The R^2 indicates the significant relationships ($n = 6-8$ trees per species).

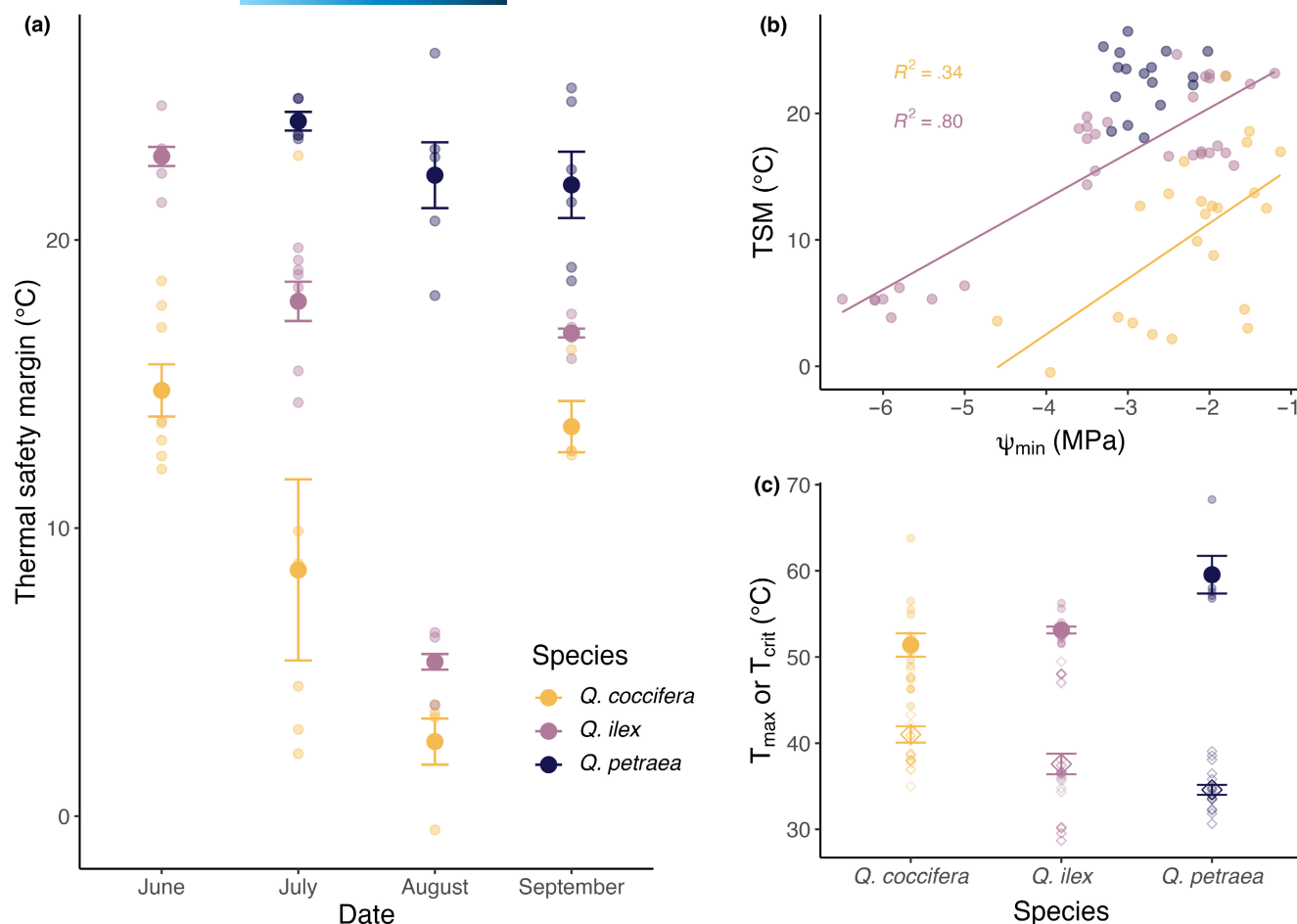


FIGURE 7 Seasonal variation in the thermal safety margins (TSM) (a), relationships between TSM and minimum water potential (b) and mean critical temperature (T_{crit} : Full point) and maximum canopy temperature over the whole growing season (T_{max} : Open symbol) (c), for *Q. coccifera* (yellow), *Q. ilex* (pink), and *Q. petraea* (dark blue). Data are means \pm SE of six (*Q. petraea*) to eight (*Q. coccifera* and *Q. ilex*) trees per species. The R^2 indicates the significant relationships ($n = 6$ –8 trees per species).

trees to maintain positive safety margins (i.e., T_{can} consistently remained under T_{crit}) (Figure 7c).

In line with our second hypothesis, A_{net} and g_s varied largely from wetter and colder to drier and hotter periods, showing a steep decrease with increasing T_{air} and decreasing soil moisture in the most southern sites that experienced extreme conditions (Figure 1; Figure S1). Indeed, *Q. coccifera* and *Q. ilex* reduced A_{net} and g_s with decreasing Ψ (Figures 2–4), indicating that trees quickly closed their stomates to avoid water loss. At the peak of the summer, we further found that trees in our two southern sites could not maintain positive A_{net} during the day, which quickly declined to values close to or below 0 when T_{can} surpassed $\sim 40^\circ\text{C}$. Nevertheless, despite important heat stress, *Q. ilex* and *Q. coccifera* sustained positive A_{net} during relatively dry periods (until ~ -4 and -3 MPa, respectively), highlighting their high heat tolerance (García-Plazaola et al., 2017). This suggests that A_{net} can be maintained under heat and moderate drought but will sharply decrease when temperatures and soil drought become extreme. Conversely, there was no relationship between Ψ and A_{net} and g_s for *Q. petraea* (Figure 4; Figure S3), suggesting that mild soil drought and high T_{air} were insufficient to induce stomatal closure for

this species. After extracting xylem vulnerability curves from the literature (Lobo et al., 2018; Pita et al., 2005; Sargent et al., 2020; Vilagrosa et al., 2003), we observed that the daily minimum Ψ reached in *Q. ilex* and *Q. petraea* were low enough to induce over 10% of embolism (Ψ_{12} in *Q. ilex* ~ -4.3 MPa and Ψ_{12} in *Q. petraea* ~ -2.2 MPa), possibly indicating that stomata remained open for photosynthesis and evaporative cooling to occur despite embolism initiation. While stomatal closure is usually observed long before xylem cavitation, previous work also observed stomata remaining open passed critical embolism thresholds when exposed either to heat alone or hot and dry conditions simultaneously (e.g., Fang et al., 2011; Schönbeck et al., 2022). Nevertheless, it is also possible that the Ψ_{50} of our individual trees were slightly lower than previously published values from the literature. Conversely, the leaf hydraulic conductance of *Q. ilex*, including the xylary water pathways, was measured to be ~ -5.4 MPa (Limousin et al., 2022). As we recorded minimum twig Ψ values around -5.9 MPa, this indicates that significant losses of leaf functions occurred in summer 2023 in FR.

Our results also showed that T_{can} was strongly correlated with T_{air} with canopies being generally warmer than the air throughout

the day. During the warmest periods, T_{can} in *Q. ilex* and *Q. coccifera* reached values up to 10°C above the air (i.e., when $T_{\text{air}} > 30^\circ\text{C}$, Figure 5). Widespread leaf scorching developed in *Q. ilex* after the heatwave (Figure S6), between our August and September campaigns, leading to widespread leaf scorching in *Q. ilex* (Figure S6). This leaf scorching developed after the heatwave between our August and September campaigns, suggesting that it may be due to the legacy effects of severe drought stress. Canopies heating up to 5°C above the air have been previously observed in *Eucalyptus parramattensis* (Drake et al., 2020), *Eucalyptus tereticornis*, and *Myristica globosa* (Crous et al., 2023) and multiple broadleaf species (Leuzinger & Körner, 2007; Scherrer et al., 2011; Still et al., 2022). However, heating up to 10°C was rarely observed before in situ (+10°C in *Quercus pannosa*, Zhou et al., 2023), except in *Cactaceae* species (+20°C in *Opuntia basilaris*, Smith, 1978). These large deviations between T_{can} and T_{air} are often observed during wind lulls on hot and sunny days and may be more common in dry environments (Gräf et al., 2021; Peguero-Pina et al., 2020). Furthermore, T_{can} was rarely regulated to values lower than T_{air} during heat peaks. These results confirm previous studies suggesting that many species do not downregulate T_{can} with increasing T_{air} (Crous et al., 2023; Doughty et al., 2023; Drake et al., 2020; Fauset et al., 2018; Sperlich et al., 2019; Still et al., 2022) despite maintaining gas exchange (i.e., A_{net} and transpiration rate) (Gauthey et al., 2023; Muller et al., 2021). We further found that *Q. ilex* and *Q. coccifera* had an anticlockwise hysteresis (i.e., canopies slightly colder than T_{air} in the morning, leading to negative ΔT , but warming faster than air during the day). This pattern is typical for sites with low leaf areas and open canopies because leaves are mostly sunlit (Law et al., 2001), and soil water depletion happens faster, resulting in higher water stress. Negative ΔT (i.e., $T_{\text{can}} - T_{\text{air}}$) corresponded mainly to morning or evening measurements (Figure S7), suggesting that foliage is colder than the air only during periods of low radiation (Miller et al., 2021; Rey-Sánchez et al., 2016).

In line with our third hypothesis, during the extreme 2023 heatwave (T_{air} reached the second highest values ever recorded at the FR site), *Q. coccifera* and *Q. ilex* decoupled A_{net} and g_s , whereby A_{net} was negative while g_s still exhibited low yet positive values (Figure 4a). There is abundant evidence reporting that g_s and A_{net} are strongly correlated under various environmental conditions (Anev et al., 2016; Hérault et al., 2013; Slot & Winter, 2017), and mathematical models based on this coupling usually predict observed values accurately (De Kauwe et al., 2013; Rogers et al., 2017). However, decoupling has been found in several studies (De Kauwe et al., 2019; Diao et al., 2024; Marchin et al., 2023; Urban et al., 2017a). For instance, de Drake et al. (2018) reported that while A_{net} was decreasing with T_{leaf} (as observed in this study, Figure 4), transpiration was maintained at T_{can} over 40°C in *Eucalyptus parramattensis* saplings. Similarly, Marchin et al. (2023) found that, regardless of water access, transpiration and g_s were much higher than model predictions, thus efficiently reducing T_{can} during heatwaves in a wide range of evergreen and deciduous species. While the mechanisms driving stomatal decoupling remain unknown, this phenomenon observed

at high temperatures in *Q. ilex* and *Q. coccifera*, could potentially be caused by residual leaf conductance (g_{res}) due to cuticular conductance and stomatal leakiness. Diao et al. (2024) also suggested that stomatal decoupling could be due to the leaf internal resistance and the change of water viscosity under high temperatures, and that the decline of A_{net} may be related to the Rubisco deactivation. Indeed, in some species, including *Q. ilex*, as T_{air} rises, g_{res} (leaf and bark minimum conductance, $g_{\text{min}} + g_{\text{bark}}$) increases as well (Billon et al., 2020; Bueno et al., 2019; Slot, Nardwattanawong, et al., 2021). Billon et al. (2020) further showed that the temperature threshold at which g_{min} sharply increases due to cuticular permeability (i.e., phase-transition temperature) was the highest in *Q. ilex* (43.8°C), which corresponds to the T_{can} at which we observed decoupling of g_s and A_{net} (August $T_{\text{can}} > 45^\circ\text{C}$). Similarly, it was recently shown that, in *Q. petraea*, g_{res} increased strongly with T_{air} (Wang et al., 2024) and that, in *Q. coccifera*, g_{res} at maximal stomatal closure was still positive despite increased water deficit (Bueno et al., 2020). Thus, while the maintenance of g_s during heatwaves through decoupling or g_{res} may not be enough to reduce significantly T_{can} , it could help restrict T_{can} from rising to detrimental values (i.e., above T_{crit}) and surpassing TSM. However, such a mechanism may also increase the risks of leaf embolism, resulting in delayed leaf scorching (Figure S6) and possible hydraulic failure (Cochard, 2021).

Several global analyses of leaf thermal limits reported that over 200 species, most plants exhibited large TSM (O'sullivan et al., 2017; Zhu et al., 2018). High leaf critical temperature (T_{crit}) in all species can partially explain this pattern in our study (Figure 7a). Indeed, while T_{air} were extremely high in the 2023 summer in the two southern sites, species-specific T_{crit} were high enough to avoid negative TSM. However, it must be noted that T_{can} may be slightly lower than some individual T_{leaf} because T_{can} averages across many leaves in the canopy, thus possibly increasing our TSM results. Still, despite positive TSM, we observed extended leaf scorching and tissue damage in *Q. ilex* (Figure S6), suggesting that cumulative heat and drought damages associated with photoinhibition (low A_{net}) may be more impactful than single heat events. Unfortunately, canopy scorching occurred between the measurement campaigns in August and September on trees that were not tracked throughout the summer, thereby not allowing us to conclude on the degree of thermal and moisture stress inducing the damage. Interestingly, we found that our measured T_{crit} values (54.7°C) lie at the higher range of previous measures (between 43 and 55°C; Zhu et al., 2018; Slot, Cala, et al., 2021; Doughty et al., 2023). This could be due to the increasing recurrence of heatwaves (Casanueva et al., 2023; Lhotka & Kysely, 2022) and higher temperatures globally. In a recent study, Ahrens et al. (2021) showed that repeated heatwaves increased significantly T_{50} (i.e., 50% of fluorescence is lost) by 3°C in *Corymbia calophylla*, indicating a degree of ecological stress memory. Contrary to our first hypothesis, T_{crit} was the highest in our most northern species, *Q. petraea*. This result is all the more surprising that *Q. petraea* had the largest surface leaf area (see Figure 5 insert), a trait usually correlated with lower thermotolerance (Valliere et al., 2023). It is possible that *Q. petraea*, the only deciduous species, displays a high T_{crit} due to quick

local acclimation to hot-dry climate (Zhu et al., 2018). Yet, T_{crit} did not significantly change between June and July, which was possibly due to low variation in maximum T_{air} ($< 5^{\circ}\text{C}$). Agreeing to our first hypothesis, this lack of acclimation resulted in a narrower TSM as the summer drought and heat intensified, especially in *Q. coccifera* and *Q. ilex*, which TSM reduced to less than 5°C in August.

Overall, this work demonstrated that canopy temperature was not strongly downregulated below T_{air} by evaporative cooling throughout the summer despite decoupling of photosynthesis and stomatal conductance. While, in FR, T_{air} reached the second highest value ever recorded in the summer of 2023, species-specific T_{crit} were high enough to avoid negative TSM and critical tissue damage. However, without acclimation of T_{crit} and with stronger VPD and heatwaves, TSM may be exceeded in the next decades, thus leading to important canopy scorching in these regions. Whether T_{crit} can acclimate to a drier and hotter climate and the role of stomatal decoupling may become essential regulatory traits to monitor as heatwaves increase in intensity and frequency. If these thresholds exceeded, it could cause significant adverse effects on plant performance, possibly accelerating vegetation mortality globally (Breshears et al., 2021; Gazol & Camarero, 2022).

AUTHOR CONTRIBUTIONS

Alice Gauthey: Conceptualization; data curation; formal analysis; investigation; methodology; project administration; writing – original draft. **Ansgar Kahmen:** Methodology; resources; writing – review and editing. **Jean-Marc Limousin:** Methodology; resources; writing – review and editing. **Alberto Vilagrosa:** Methodology; resources; writing – review and editing. **Margaux Didion-Gency:** Investigation; writing – review and editing. **Eugénie Mas:** Investigation; writing – review and editing. **Alex Tunas:** Investigation; writing – review and editing. **Arianna Milano:** Investigation; methodology. **Charlotte Grossiord:** Conceptualization; funding acquisition; investigation; methodology; writing – review and editing.

ACKNOWLEDGMENTS

AG and CG were supported by the Sandoz Family Foundation. CG was further supported by the Swiss National Science Foundation SNSF (310030_204697). The Puéchabon experimental site belongs to the French national research infrastructure ANAEE-France (ANR-11-INBS-0001) and the French network of ICOS Ecosystem stations (Integrated Carbon Observation. System ERIC). We thank Omar Basquet, Jean Kempf, Jolan Wicht, Arianna Milano, Maxwell Bergstrom, and Niek Abram ten Cate for contributing to the data collection. We also thank Sociedad de Cazadores de Muro (Alicante) for their facilities during field samplings. AV was supported by the INERTIA project (PID2019-111332RB-C22) and EVER project (CIPROM/2022/37–Promete program). CEAM is funded by Generalitat Valenciana.

CONFLICT OF INTEREST STATEMENT

None declared.

DATA AVAILABILITY STATEMENT

The data that support the findings of this study are openly available in the Dryad Digital Repository at <https://datadryad.org/stash/share/tGYEQjeJTyipAjlrr7Okh4i2NAcPI0zKlIttBsIvECOL>.

ORCID

Alice Gauthey  <https://orcid.org/0000-0002-4432-8249>

Eugénie Mas  <https://orcid.org/0009-0008-1615-7738>

Charlotte Grossiord  <https://orcid.org/0000-0002-9113-3671>

REFERENCES

- Ahrens, C. W., Challis, A., Byrne, M., Leigh, A., Nicotra, A. B., Tissue, D., & Rymer, P. (2021). Repeated extreme heatwaves result in higher leaf thermal tolerances and greater safety margins. *New Phytologist*, 232(3), 1212–1225.
- Anev, S., Marinova, A., Tzvetkova, N., Panayotov, M., & Yurukov, S. (2016). Stomatal control on photosynthesis in drought-treated sub-alpine pine saplings. *Genetics and Plant Physiology*, 6, 43–53.
- Bates, D. M. (2010). *lme4: Mixed-Effects Modeling With R*.
- Billon, L. M., Blackman, C. J., Cochard, H., Badel, E., Hitmi, A., Cartailleur, J., Souchal, R., & Torres-Ruiz, J. M. (2020). The DroughtBox: A new tool for phenotyping residual branch conductance and its temperature dependence during drought. *Plant, Cell & Environment*, 43, 1584–1594.
- Bréda, N., Huc, R., Granier, A., & Dreyer, E. (2006). Temperate forest trees and stands under severe drought: A review of ecophysiological responses, adaptation processes and long-term consequences. *Annals of Forest Science*, 63, 625–644.
- Breshears, D. D., Fontaine, J. B., Ruthrof, K. X., Field, J. P., Feng, X., Burger, J. R., Law, D. J., Kala, J., & Hardy, G. E. S. J. (2021). Underappreciated plant vulnerabilities to heat waves. *New Phytologist*, 231, 32–39.
- Bueno, A., Alfarhan, A., Arand, K., Burghardt, M., Deininger, A.-C., Hedrich, R., Leide, J., Seufert, P., Staiger, S., & Riederer, M. (2019). Effects of temperature on the cuticular transpiration barrier of two desert plants with water-spender and water-saver strategies. *Journal of Experimental Botany*, 70, 1613–1625.
- Bueno, A., Sancho-Knapik, D., Gil-Pelegrin, E., Leide, J., Peguero-Pina, J. J., Burghardt, M., & Riederer, M. (2020). Cuticular wax coverage and its transpiration barrier properties in *Quercus coccifera* L. leaves: Does the environment matter? *Tree Physiology*, 40(7), 827–840.
- Casanueva, A., Kotlarski, S., Liniger, M. A., Schwierz, C., & Fischer, A. M. (2023). Climate change scenarios in use: Heat stress in Switzerland. *Climate Services*, 30, 100372.
- Coast, O., Posch, B. C., Rognoni, B. G., Bramley, H., Gaju, O., Mackenzie, J., Pickles, C., Kelly, A. M., Lu, M., Ruan, Y.-L., Trethowan, R., & Atkin, O. K. (2022). Wheat photosystem II heat tolerance: Evidence for genotype-by-environment interactions. *The Plant Journal*, 111, 1368–1382.
- Cochard, H. (2021). A new mechanism for tree mortality due to drought and heatwaves. *Peer Community Journal*, 1, e36.
- Cook, A. M., Berry, N., Milner, K. V., & Leigh, A. (2021). Water availability influences thermal safety margins for leaves. *Functional Ecology*, 35, 2179–2189.
- Cook, A. M., Rezende, E. L., Petrou, K., & Leigh, A. (2024). Beyond a single temperature threshold: Applying a cumulative thermal stress framework to plant heat tolerance. *Ecology Letters*, 27, e14416.
- Copernicus Climate Change Service/ECMWF. (2023). *Copernicus Climate Change Service/ECMWF Surface air temperature for August 2023*. Copernicus.
- Crous, K. Y., Cheesman, A. W., Middleby, K., Rogers, E. I. E., Wujeska-Klaue, A., Bouet, A. Y. M., Ellsworth, D. S., Liddell, M. J., Cernusak, L. A., & Barton, C. V. M. (2023). Similar patterns of leaf temperatures

- and thermal acclimation to warming in temperate and tropical tree canopies (M Cavaleri, Ed.). *Tree Physiology*, 43, 1383–1399.
- Curtis, E. M., Gollan, J., Murray, B. R., & Leigh, A. (2016). Native microhabitats better predict tolerance to warming than latitudinal macro-climatic variables in arid-zone plants. *Journal of Biogeography*, 43, 1156–1165.
- De Kauwe, M. G., Medlyn, B. E., Pitman, A. J., Drake, J. E., Ukkola, A., Griebel, A., Pendall, E., Prober, S., & Roderick, M. (2019). Examining the evidence for decoupling between photosynthesis and transpiration during heat extremes. *Biogeosciences*, 16, 903–916.
- De Kauwe, M. G., Medlyn, B. E., Zaehle, S., Walker, A. P., Dietze, M. C., Hickler, T., Jain, A. K., Luo, Y., Parton, W. J., Prentice, I. C., Smith, B., Thornton, P. E., Wang, S., Wang, Y. P., Wärlind, D., Weng, E., Crous, K. Y., Ellsworth, D. S., Hanson, P. J., ... Norby, R. J. (2013). Forest water use and water use efficiency at elevated CO₂: A model-data intercomparison at two contrasting temperate forest FACE sites. *Global Change Biology*, 19, 1759–1779.
- Diao, H., Cernusak, L. A., Saurer, M., Gessler, A., Siegwolf, R. T. W., & Lehmann, M. M. (2024). Uncoupling of stomatal conductance and photosynthesis at high temperatures: Mechanistic insights from online stable isotope techniques. *New Phytologist*, 241, 2366–2378.
- Doughty, C. E., Keany, J. M., Wiebe, B. C., Rey-Sanchez, C., Carter, K. R., Middleby, K. B., Cheesman, A. W., Goulden, M. L., da Rocha, H. R., Miller, S. D., Malhi, Y., Fauset, S., Gloor, E., Slot, M., Oliveras Menor, I., Crous, K. Y., Goldsmith, G. R., & Fisher, J. B. (2023). Tropical forests are approaching critical temperature thresholds. *Nature*, 621, 105–111.
- Drake, J. E., Harwood, R., Vårhammar, A., Barbour, M. M., Reich, P. B., Barton, C. V. M., & Tjoelker, M. G. (2020). No evidence of homeostatic regulation of leaf temperature in *Eucalyptus parramattensis* trees: Integration of CO₂ flux and oxygen isotope methodologies. *New Phytologist*, 228, 1511–1523.
- Drake, J. E., Tjoelker, M. G., Vårhammar, A., Medlyn, B. E., Reich, P. B., Leigh, A., Pfautsch, S., Blackman, C. J., López, R., Aspinwall, M. J., Crous, K. Y., Duursma, R. A., Kumarathunge, D., de Kauwe, M. G., Jiang, M., Nicotra, A. B., Tissue, D. T., Choat, B., Atkin, O. K., & Barton, C. V. M. (2018). Trees tolerate an extreme heatwave via sustained transpirational cooling and increased leaf thermal tolerance. *Global Change Biology*, 24, 2390–2402.
- Eamus, D., Boulain, N., Cleverly, J., & Breshears, D. D. (2013). Global change-type drought-induced tree mortality: Vapor pressure deficit is more important than temperature per se in causing decline in tree health. *Ecology and Evolution*, 3, 2711–2729.
- Esperon-Rodriguez, M., Baumgartner, J. B., Beaumont, L. J., Lenoir, J., Nipperess, D., Power, S. A., Richard, B., Rymer, P. D., Tjoelker, M. G., & Gallagher, R. V. (2021). Climate-change risk analysis for global urban forests. *bioRxiv*, 2021-05. <https://doi.org/10.1101/2021.05.09.444303>
- Fang, X., Turner, N., Li, F.-M., Li, W., & Guo, X. (2011). *Caragana korshinskii* seedlings maintain positive photosynthesis during short-term, severe drought stress. *Photosynthetica*, 49, 603–609.
- Fauset, S., Freitas, H. C., Galbraith, D. R., Sullivan, M. J. P., Aidar, M. P. M., Joly, C. A., Phillips, O. L., Vieira, S. A., & Gloor, M. U. (2018). Differences in leaf thermoregulation and water use strategies between three co-occurring Atlantic forest tree species. *Plant, Cell & Environment*, 41, 1618–1631.
- García-Fórner, N., Adams, H. D., Servanto, S., Collins, A. D., Dickman, L. T., Hudson, P. J., Zeppel, M. J. B., Jenkins, M. W., Powers, H., Martínez-Vilalta, J., & McDowell, N. G. (2016). Responses of two semiarid conifer tree species to reduced precipitation and warming reveal new perspectives for stomatal regulation. *Plant, Cell & Environment*, 39, 38–49.
- García-Plazaola, J. I., Hernández, A., Fernández-Marín, B., Esteban, R., Peguero-Pina, J. J., Verhoeven, A., & Cavender-Bares, J. (2017). Photoprotective mechanisms in the genus *Quercus* in response to winter cold and summer drought. In E. Gil-Pelegrín, J. J. Peguero-Pina, & D. Sancho-Knapik (Eds.), *Tree physiology. Oaks physiological ecology. Exploring the functional diversity of genus Quercus L* (pp. 361–391). Springer International Publishing.
- Gauthey, A., Bachofen, C., Deluigi, J., Didion-Gency, M., D'Odorico, P., Gisler, J., Mas, E., Schaub, M., Schuler, P., Still, C. J., Tunas, A., & Grossiord, C. (2023). Absence of canopy temperature variation despite stomatal adjustment in *Pinus sylvestris* under multidecadal soil moisture manipulation. *New Phytologist*, 240, 127–137.
- Gazol, A., & Camarero, J. J. (2022). Compound climate events increase tree drought mortality across European forests. *Science of the Total Environment*, 816, 151604.
- Gong, X.-W., & Hao, G.-Y. (2023). The synergistic effect of hydraulic and thermal impairments accounts for the severe crown damage in *Fraxinus mandshurica* seedlings following the combined drought-heatwave stress. *Science of the Total Environment*, 856, 159017.
- Gräf, M., Immitzer, M., Hietz, P., & Stangl, R. (2021). Water-stressed plants do not cool: Leaf surface temperature of living wall plants under drought stress. *Sustainability*, 13, 3910.
- Grossiord, C., Buckley, T. N., Cernusak, L. A., Novick, K. A., Poulter, B., Siegwolf, R. T. W., Sperry, J. S., & McDowell, N. G. (2020). Plant responses to rising vapor pressure deficit. *New Phytologist*, 226, 1550–1566.
- Hammond, W. M., Williams, A. P., Abatzoglou, J. T., Adams, H. D., Klein, T., López, R., Sáenz-Romero, C., Hartmann, H., Breshears, D. D., & Allen, C. D. (2022). Global field observations of tree die-off reveal hotter-drought fingerprint for Earth's forests. *Nature Communications*, 13, 1761.
- Harrap, M. J. M., Hempel De Ibarra, N., Whitney, H. M., & Rands, S. A. (2018). Reporting of thermography parameters in biology: A systematic review of thermal imaging literature. *Royal Society Open Science*, 5, 181281.
- Hérault, A., Lin, Y.-S., Bourne, A., Medlyn, B. E., & Ellsworth, D. S. (2013). Optimal stomatal conductance in relation to photosynthesis in climatically contrasting eucalyptus species under drought. *Plant, Cell & Environment*, 36, 262–274.
- Hüve, K., Bichele, I., Rasulov, B., & Niinemets, Ü. (2011). When it is too hot for photosynthesis: Heat-induced instability of photosynthesis in relation to respiratory burst, cell permeability changes and H₂O₂ formation. *Plant, Cell & Environment*, 34, 113–126.
- Intergovernmental Panel On Climate Change. (2023). *Climate change 2021 – The physical science basis: Working group I contribution to the sixth assessment report of the intergovernmental panel on climate change*. Cambridge University Press.
- Kahmen, A., Basler, D., Hoch, G., Link, R. M., Schuldt, B., Zahnd, C., & Arend, M. (2022). Root water uptake depth determines the hydraulic vulnerability of temperate European tree species during the extreme 2018 drought. *Plant Biology*, 24, 1224–1239.
- Kattenborn, T. (2023). *DJI thermal rpeg to tif* (v. 0.5).
- Kitudom, N., Fauset, S., Zhou, Y., Fan, Z., Li, M., He, M., Zhang, S., Xu, K., & Lin, H. (2022). Thermal safety margins of plant leaves across biomes under a heatwave. *Science of the Total Environment*, 806, 150416.
- Klein, T. (2014). The variability of stomatal sensitivity to leaf water potential across tree species indicates a continuum between isohydric and anisohydric behaviours. *Functional Ecology*, 28(6), 1313–1320.
- Krause, G. H., Winter, K., Krause, B., Jahns, P., García, M., Aranda, J., & Virgo, A. (2010). High-temperature tolerance of a tropical tree, *Ficus insipida*: Methodological reassessment and climate change considerations. *Functional Plant Biology*, 37, 890–900.
- Kullberg, A. T., Coombs, L., Soria Ahuanari, R. D., Fortier, R. P., & Feeley, K. J. (2024). Leaf thermal safety margins decline at hotter temperatures in a natural warming 'experiment' in the Amazon. *New Phytologist*, 241, 1447–1463.
- Lancaster, L. T., & Humphreys, A. M. (2020). Global variation in the thermal tolerances of plants. *Proceedings of the National Academy of Sciences of the United States of America*, 117, 13580–13587.
- Law, B. E., Cescatti, A., & Baldocchi, D. D. (2001). Leaf area distribution and radiative transfer in open-canopy forests: Implications for mass and energy exchange. *Tree Physiology*, 21, 777–787.

- Leuzinger, S., & Körner, C. (2007). Tree species diversity affects canopy leaf temperatures in a mature temperate forest. *Agricultural and Forest Meteorology*, 146, 29–37.
- Lhotka, O., & Kyselý, J. (2022). The 2021 European heat wave in the context of past major heat waves. *Earth and Space Science*, 9, e2022EA002567.
- Limousin, J.-M., Roussel, A., Rodríguez-Calcerrada, J., Torres-Ruiz, J. M., Moreno, M., García de Jalon, L., Ourcival, J.-M., Simioni, G., Cochard, H., & Martin-StPaul, N. (2022). Drought acclimation of *Quercus ilex* leaves improves tolerance to moderate drought but not resistance to severe water stress. *Plant, Cell & Environment*, 45, 1967–1984.
- Lobo, A., Torres-Ruiz, J. M., Burlett, R., Lemaire, C., Parise, C., Francioni, C., Truffaut, L., Tomášková, I., Hansen, J. K., Kjær, E. D., Kremer, A., & Delzon, S. (2018). Assessing inter- and intraspecific variability of xylem vulnerability to embolism in oaks. *Forest Ecology and Management*, 424, 53–61.
- Marchin, R. M., Backes, D., Ossola, A., Leishman, M. R., Tjoelker, M. G., & Ellsworth, D. S. (2022). Extreme heat increases stomatal conductance and drought-induced mortality risk in vulnerable plant species. *Global Change Biology*, 28, 1133–1146.
- Marchin, R. M., Broadhead, A. A., Bostic, L. E., Dunn, R. R., & Hoffmann, W. A. (2016). Stomatal acclimation to vapour pressure deficit doubles transpiration of small tree seedlings with warming. *Plant, Cell & Environment*, 39, 2221–2234.
- Marchin, R. M., Medlyn, B. E., Tjoelker, M. G., & Ellsworth, D. S. (2023). Decoupling between stomatal conductance and photosynthesis occurs under extreme heat in broadleaf tree species regardless of water access. *Global Change Biology*, 29, 6319–6335.
- Miller, B. D., Carter, K. R., Reed, S. C., Wood, T. E., & Cavaleri, M. A. (2021). Only sun-lit leaves of the uppermost canopy exceed both air temperature and photosynthetic thermal optima in a wet tropical forest. *Agricultural and Forest Meteorology*, 301, 108347.
- Moran, M. E., Aparecido, L. M. T., Koepke, D. F., Cooper, H. F., Doughty, C. E., Gehring, C. A., Throop, H. L., Whitham, T. G., Allan, G. J., & Hultine, K. R. (2023). Limits of thermal and hydrological tolerance in a foundation tree species (*Populus fremontii*) in the desert southwestern United States. *New Phytologist*, 240, 2298–2311.
- Muller, J. D., Rotenberg, E., Tatarinov, F., Oz, I., & Yakir, D. (2021). Evidence for efficient nonevaporative leaf-to-air heat dissipation in a pine forest under drought conditions. *New Phytologist*, 232, 2254–2266.
- O'sullivan, O. S., Heskell, M. A., Reich, P. B., Tjoelker, M. G., Weerasinghe, L. K., Penillard, A., Zhu, L., Egerton, J. J. G., Bloomfield, K. J., Creek, D., Bahar, N. H., Griffin, K. L., Hurry, V., Meir, P., Turnbull, M. H., & Atkin, O. K. (2017). Thermal limits of leaf metabolism across biomes. *Global Change Biology*, 23, 209–223.
- Peguero-Pina, J. J., Vilagrosa, A., Alonso-Forn, D., Ferrio, J. P., Sancho-Knapik, D., & Gil-Pelegrín, E. (2020). Living in drylands: Functional adaptations of trees and shrubs to cope with high temperatures and water scarcity. *Forests*, 11, 1028.
- Pita, P., Cañas, I., Soria, F., Ruiz, F., & Toval, G. (2005). Use of physiological traits in tree breeding for improved yield in drought-prone environments. The case of *Eucalyptus globulus*. *Investigación Agraria. Sistemas y Recursos Forestales*, 14, 383–393.
- Rey-Sánchez, A., Slot, M., Posada, J., & Kitajima, K. (2016). Spatial and seasonal variation in leaf temperature within the canopy of a tropical forest. *Climate Research*, 71, 75–89.
- Rogers, A., Medlyn, B. E., Dukes, J. S., Bonan, G., von Caemmerer, S., Dietze, M. C., Kattge, J., Leakey, A. D. B., Mercado, L. M., Niinemets, Ü., Prentice, I. C., Serbin, S. P., Sitch, S., Way, D. A., & Zaehle, S. (2017). A roadmap for improving the representation of photosynthesis in earth system models. *New Phytologist*, 213, 22–42.
- RStudio Team. (2015). *RStudio: Integrated development for R*. RStudio, Inc. <http://www.rstudio.com/>
- Sastry, A., Guha, A., & Barua, D. (2018). Leaf thermotolerance in dry tropical forest tree species: Relationships with leaf traits and effects of drought. *AoB Plants*, 10(1), plx070.
- Scherrer, D., Bader, M. K.-F., & Körner, C. (2011). Drought-sensitivity ranking of deciduous tree species based on thermal imaging of forest canopies. *Agricultural and Forest Meteorology*, 151, 1632–1640.
- Schönbeck, L., Schuler, P., Lehmann, M. M., Mas, E., Mekarni, L., Pivovarov, A. L., Turberg, P., & Grossiord, C. (2022). Increasing temperature and vapour pressure deficit lead to hydraulic damages in the absence of soil drought. *Plant, Cell & Environment*, 45, 3275–3289.
- Sergeant, A. S., Varela, S. A., Barigah, T. S., Badel, E., Cochard, H., Dalla-Salda, G., Delzon, S., Fernández, M. E., Guillemot, J., Gyenge, J., Lamarque, L. J., Martinez-Meier, A., Rozenberg, P., Torres-Ruiz, J. M., & Martin-StPaul, N. K. (2020). A comparison of five methods to assess embolism resistance in trees. *Forest Ecology and Management*, 468, 118175.
- Slot, M., Cala, D., Aranda, J., Virgo, A., Michalet, S. T., & Winter, K. (2021). Leaf heat tolerance of 147 tropical forest species varies with elevation and leaf functional traits, but not with phylogeny. *Plant, Cell & Environment*, 44, 2414–2427.
- Slot, M., Nardwattanawong, T., Hernández, G. G., Bueno, A., Riederer, M., & Winter, K. (2021). Large differences in leaf cuticle conductance and its temperature response among 24 tropical tree species from across a rainfall gradient. *New Phytologist*, 232, 1618–1631.
- Slot, M., & Winter, K. (2017). In situ temperature response of photosynthesis of 42 tree and liana species in the canopy of two Panamanian lowland tropical forests with contrasting rainfall regimes. *New Phytologist*, 214, 1103–1117.
- Smith, W. K. (1978). Temperatures of desert plants: Another perspective on the adaptability of leaf size. *Science*, 201, 614–616.
- Sperlich, D., Chang, C. T., Peñuelas, J., & Sabaté, S. (2019). Responses of photosynthesis and component processes to drought and temperature stress: Are Mediterranean trees fit for climate change? *Tree Physiology*, 39, 1783–1805.
- Still, C. J., Page, G., Rastogi, B., Griffith, D. M., Aubrecht, D. M., Kim, Y., Burns, S. P., Hanson, C. V., Kwon, H., Hawkins, L., Meinzer, F. C., Sevanto, S., Roberts, D., Goulden, M., Pau, S., Detto, M., Helliker, B., & Richardson, A. D. (2022). No evidence of canopy-scale leaf thermoregulation to cool leaves below air temperature across a range of forest ecosystems. *Proceedings of the National Academy of Sciences of the United States of America*, 119, e2205682119.
- Urban, J., Ingwers, M., McGuire, M. A., & Teskey, R. O. (2017b). Stomatal conductance increases with rising temperature. *Plant Signaling & Behavior*, 12, e1356534.
- Urban, J., Ingwers, M. W., McGuire, M. A., & Teskey, R. O. (2017a). Increase in leaf temperature opens stomata and decouples net photosynthesis from stomatal conductance in *Pinus taeda* and *Populus deltoides* x *nigra*. *Journal of Experimental Botany*, 68, 1757–1767.
- Valliere, J. M., Nelson, K. C., & Martinez, M. C. (2023). Functional traits and drought strategy predict leaf thermal tolerance. *Conservation Physiology*, 11, coad085.
- Vilagrosa, A., Bellot, J., Vallejo, V. R., & Gil-Pelegrín, E. (2003). Cavitation, stomatal conductance, and leaf dieback in seedlings of two co-occurring Mediterranean shrubs during an intense drought. *Journal of Experimental Botany*, 54, 2015–2024.
- Wang, S., Hoch, G., Grun, G., & Kahmen, A. (2024). Water loss after stomatal closure: Quantifying leaf minimum conductance and minimal water use in nine temperate European tree species during a severe drought. *Tree Physiology*, 44, tpae027.
- Will, R. E., Wilson, S. M., Zou, C. B., & Hennessey, T. C. (2013). Increased vapor pressure deficit due to higher temperature leads to greater transpiration and faster mortality during drought for tree seedlings common to the forest-grassland ecotone. *New Phytologist*, 200, 366–374.
- Williams, A. P., Allen, C. D., Macalady, A. K., Griffin, D., Woodhouse, C. A., Meko, D. M., Swetnam, T. W., Rauscher, S. A., Seager, R., Grissino-Mayer, H. D., Dean, J. S., Cook, E. R., Gangodagamage, C., Cai, M., & McDowell, N. G. (2013). Temperature as a potent driver of regional forest drought stress and tree mortality. *Nature Climate Change*, 3, 292–297.

- Wilson, K. B., Baldocchi, D. D., Aubinet, M., Berbigier, P., Bernhofer, C., Dolman, H., Falge, E., Field, C., Goldstein, A., Granier, A., Grelle, A., Halldor, T., Hollinger, D., Katul, G., Law, B. E., Lindroth, A., Meyers, T., Moncrieff, J., Monson, R., ... Wofsy, S. (2002). Energy partitioning between latent and sensible heat flux during the warm season at FLUXNET sites. *Water Resources Research*, 38, 1–11.
- Zhou, Y., Kitudom, N., Fauset, S., Slot, M., Fan, Z., Wang, J., Liu, W., & Lin, H. (2023). Leaf thermal regulation strategies of canopy species across four vegetation types along a temperature and precipitation gradient. *Agricultural and Forest Meteorology*, 343, 109766.
- Zhu, L., Bloomfield, K. J., Hocart, C. H., Egerton, J. J. G., O'Sullivan, O. S., Penillard, A., Weerasinghe, L. K., & Atkin, O. K. (2018). Plasticity of photosynthetic heat tolerance in plants adapted to thermally contrasting biomes. *Plant, Cell & Environment*, 41, 1251–1262.

SUPPORTING INFORMATION

Additional supporting information can be found online in the Supporting Information section at the end of this article.

How to cite this article: Gauthey, A., Kahmen, A., Limousin, J.-M., Vilagrosa, A., Didion-Gency, M., Mas, E., Milano, A., Tunas, A., & Grossiord, C. (2024). High heat tolerance, evaporative cooling, and stomatal decoupling regulate canopy temperature and their safety margins in three European oak species. *Global Change Biology*, 30, e17439. <https://doi.org/10.1111/gcb.17439>